Macromolecules
COMMUNICATION TO THE EDITOR

Macromolecules **2010**, *43*, 3161–3164 **3161**
DOI: 10.1021/ma100192n

Sequence Fractionation in Symmetric Random Block Copolymers

Alice von der Heydt,* Marcus Müller, and Annette Zippelius

Institut für Theoretische Physik, Universität Göttingen, Friedrich-Hund-Platz 1, 37077 Göttingen, Germany

Received January 25, 2010
Revised Manuscript Received February 22, 2010

Introduction. Analytically calculated mean-field phase diagrams of symmetric, random A−B block copolymer melts reveal a new topology at the transition from macro- to microphase separation. In the plane of block type correlation and incompatibility, (λ, χ), we identify a coexistence region of two macroscopic A- and B-rich phases and one lamellar (micro)phase. The three coexisting phases display fractionation, i.e., sequence distributions deviating from the global, λ-defined one: alternating sequences accumulate in the lamellae, homopolymers prefer the macroscopic phases. Regions of pure macroscopic vs pure lamellar phase separation flank the coexistence region and meet in a multicritical point, whose nature for triblocks depends on the number M of identical segments per block.

Already in binary block copolymers with one fixed sequence, built of incompatible monomer types A and B, the competition between conformational entropy, connectedness of A and B, incompressibility, and incompatibility results in complex phases.[1−5] Random multiblock copolymers with a *distribution* of block sequences show an even richer behavior.[3,4,6−12] With increasing incompatibility,[13] separations into a growing number of macroscopic phases of different compositions are predicted by classifying chains solely according to their A content.[6,14,15] Chains' internal structure and thus the possibility of microphase separation[3,4,16] have been considered by Fredrickson et al.,[3,4] who derive a Landau−Wilson free energy cost associated with A density modulations. Three phases occur in the symmetric system: The line of instabilities of the homogeneously mixed, disordered phase is divided into two parts by an isotropic Lifshitz point[17,18] at the block type correlation λ_c: on crossing the line by increasing the incompatibility, the melt separates into macroscopic phases with zero wavenumber for correlations $\lambda > \lambda_c$ and into spatially structured microphases with finite wavenumber for $\lambda < \lambda_c$. Still, the route from macroscopic to microphase separation remained unclear.

Our mean-field treatment of lamellar phase separation in the weak segregation limit is based on the model of ref 4, but with account for individual *sequences* and without the many-block approximation. Combined with the exact macroscopic phase separation amplitude, we analyze a minimal model for the *coexistence* of homogeneous and spatially structured phases enabled by sequence-specific fractionation. With this focus, we shall not enter the controversial debate on the effect of order parameter fluctuations[19,20] on the transition to and the stability of pure microphases.[7,21−23] Fractionated three-phase coexistence was found in diblock−homopolymer blends[24] and suggested also for symmetric random triblock copolymers in simulations.[25,26] Details of the present approach, compared to results from self-consistent field calculations, will follow.[27]

Model. We consider an incompressible melt of N linear, random A−B block copolymers. All chains have $L = QM$ segments, divided into Q blocks, composed of M segments of one type each:

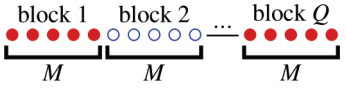

A binary variable $q_j(s)$ parametrizes the type of segment s on chain j, taking the values +1 for type A and −1 for type B. The block sequences stem from a Markovian polymerization process with average A content $^1/_2$ and block type correlation $\lambda \in [-1, 1]$:[4]

$$\lambda = \begin{cases} +1: & \text{homopolymers only, e.g. } \blacksquare\blacksquare\blacksquare\cdots, \\ 0: & \text{ideal random sequences with uncorrelated blocks,} \\ -1: & \text{strictly alternating seq. only, e.g. } \blacksquare\square\blacksquare\cdots \end{cases}$$

Once generated, they are fixed.

Order Parameter and Hamiltonian. The order parameters are the local A excess,[4,28] signaling A−B separation[29]

$$\sigma(\mathbf{r}) = \sum_{j=1}^{N}\sum_{s=1}^{L} q_j(s)\delta(\mathbf{r}-\mathbf{r}_j(s)) = \rho_A(\mathbf{r}) - \rho_B(\mathbf{r}) \qquad (1)$$

and the local segment density, $\rho(\mathbf{r}) = \rho_A(\mathbf{r}) + \rho_B(\mathbf{r})$. The Hamiltonian, $\mathscr{H} = \mathscr{H}_W + \mathscr{H}_\kappa + \mathscr{H}_\chi$, consists of the bonded interaction $\mathscr{H}_W$ within a Gaussian chain, the compressibility and the incompatibility, in units of k_BT:

$$\mathscr{H}_\kappa = \frac{\kappa}{4\rho_0}\int \mathrm{d}^d r \;\; (\rho(\mathbf{r}) - \rho_0)^2 \qquad (2a)$$

$$\mathscr{H}_\chi = -\frac{\chi}{4\rho_0}\int \mathrm{d}^d r \;\; \sigma^2(\mathbf{r}) \qquad (2b)$$

Lengths are measured in units of the statistical segment length, κ is the compression modulus, and $\rho_0 = NL/V$ is the average segment density. The zero of the incompatibility interaction is the homogeneously mixed state, $\rho_A = \rho_B = \rho_0/2$.

Free Energy. The canonical partition function, $\mathscr{Z}$, is expressed in terms of σ and ρ, $\mathscr{Z} = \int \mathscr{D}\rho_{\mathbf{k}} \mathscr{D}\sigma_{\mathbf{k}} \exp\{-Nh(\{\rho_{\mathbf{k}}, \sigma_{\mathbf{k}}\})\}$.[27] The conformational weight with $\mathscr{H}_W$ factorizes with respect to chains, all chains of one sequence ν producing the same factor, such that the effective Hamiltonian h per chain contains single-sequence partition functions z_ν:

$$h = -\frac{1}{4N^2L}\sum_{\mathbf{k}\neq 0}(\kappa\rho_{\mathbf{k}}\rho_{-\mathbf{k}} - \chi\sigma_{\mathbf{k}}\sigma_{-\mathbf{k}}) - \sum_\nu p_\nu\left(\ln\frac{z_\nu}{p_\nu} + 1\right)$$

$$z_\nu = \int \mathscr{D}\mathbf{r}(s)\mathrm{e}^{-\mathscr{H}_W}\exp\left\{\frac{1}{2NL}\sum_{\mathbf{k}\neq 0,s}(\chi q_\nu(s)\sigma_{\mathbf{k}} - \kappa\rho_{\mathbf{k}})\mathrm{e}^{-i\mathbf{k}\cdot\mathbf{r}(s)}\right\} \qquad (3)$$

p_ν being the probability of a particular sequence ν characterized by $\{q_\nu(s)\}$. After eliminating $\{\rho_{\mathbf{k}}\}$ in favor of $\{\sigma_{\mathbf{k}}\}$ in the incompressible limit $\kappa \to \infty$, the free energy reduction is

*To whom correspondence should be addressed. E-mail: heydt@theorie.physik.uni-goettingen.de.

© 2010 American Chemical Society

Published on Web 03/12/2010

derived by parameter optimization of a suitable A−B modulation with amplitude $\sigma_{\mathbf{k}}$ at wavevector $\mathbf{k}$.

Lamellar Phase Separation. The simplest ansatz of a lamellar microphase

$$\sigma_{\mathbf{k}} = \sigma_0(\delta_{\mathbf{k},\mathbf{k}_0} + \delta_{\mathbf{k},-\mathbf{k}_0}) \tag{4}$$

featuring a single wavevector, is inserted into an expansion of eq 3 up to fourth order in $\sigma_{\mathbf{k}}$, with the wavenumber dependence in the coefficient of the quartic term ignored.[27] Lamellae are expected to destabilize the disordered state, if the optimal wavenumber k_0, the maximum position of the second-order structure function[30]

$$S(k^2) := \sum_{\nu} p_{\nu,\mathrm{lam}} \sum_{s_1,s_2=1}^{L} q_\nu(s_1) q_\nu(s_2) \mathrm{e}^{-k^2|s_2-s_1|} \tag{5}$$

is nonzero. With the system-spanning, λ-defined sequence distribution, $p_{\nu,\mathrm{lam}} = p_\nu(\lambda)$, this happens only for $\lambda < \lambda_c$.[4] In a subsystem, i.e., with fractionation, lamellae may occur also for $\lambda > \lambda_c$. Optimization of the free energy with respect to the amplitude σ_0 gives

$$f_{\mathrm{lam}} = -\frac{\left(\frac{S(k_0{}^2)}{L^2} - \frac{2}{L\chi}\right)^2}{q_2{}^2 + q_4} + \sum_{\nu} p_{\nu,\mathrm{lam}}(\ln p_{\nu,\mathrm{lam}} - 1) \tag{6}$$

provided $\chi \geq 2L/S(k_0{}^2)$. Here, q_2 and q_4 are the second and fourth type moments for a given distribution $\{p_{\nu,\mathrm{lam}}\}$.

The following specialization to symmetric random triblocks, $Q = 3$, requires to distinguish three classes of *sequences* with different structure functions: p_1 is the concentration of homopolymers, comprising AAA and BBB sequences, p_2 that of both AAB and BBA, and p_3 that of ABA and BAB sequences. Differentiation of the A- or B-rich subspecies is unnecessary due to the symmetry of the two phases in a macroscopically separated state.

Macroscopic Phase Separation. An ansatz of two equally sized macroscopic phases with homogeneous compositions σ_{h} and $-\sigma_{\mathrm{h}}$ yields exact in σ_{h}:

$$f_{\mathrm{h}} = \frac{L\chi\sigma_{\mathrm{h}}{}^2}{4\rho_0{}^2} - p_{1,\mathrm{h}} \ln\cosh\frac{L\chi\sigma_{\mathrm{h}}}{2\rho_0} - (1-p_{1,\mathrm{h}}) \ln\cosh\frac{L\chi\sigma_{\mathrm{h}}}{6\rho_0} + \sum_{\nu} p_{\nu,\mathrm{h}}\left(\ln p_{\nu,\mathrm{h}} - 1\right) \tag{7}$$

$$\frac{\sigma_{\mathrm{h}}}{\rho_0} = p_{1,\mathrm{h}} \tanh\frac{L\chi\sigma_{\mathrm{h}}}{2\rho_0} + \frac{1-p_{1,\mathrm{h}}}{3}\tanh\frac{L\chi\sigma_{\mathrm{h}}}{6\rho_0}, \quad \chi \geq \frac{2}{Lq_2}$$

Fractionation Ansatz. To assess three-phase coexistence with sequence-specific exchange, our explicit fractionation ansatz starts from a weighted sum of the free energies of one lamellar phase, f_{lam}, with volume fraction v, and that of two homogeneous, homopolymer-rich phases, f_{h}, with a joint volume fraction $1 - v$:

$$f_{\mathrm{fract}} := v f_{\mathrm{lam}}(\{p_{\nu,\mathrm{lam}}\}) + (1-v) f_{\mathrm{h}}(\{p_{\nu,\mathrm{h}}\}) \tag{8}$$

We optimize the free energy difference relative to *one* phase-separated structure in the entire system, macroscopic phases at $\lambda > \lambda_c$, lamellae at $\lambda < \lambda_c$. The variational parameters are the volume fraction and two sequence concentrations of the new phase, due to the constraint $v p_{\nu,\mathrm{lam}} + (1-v) p_{\nu,\mathrm{h}} = p_\nu(\lambda)$.

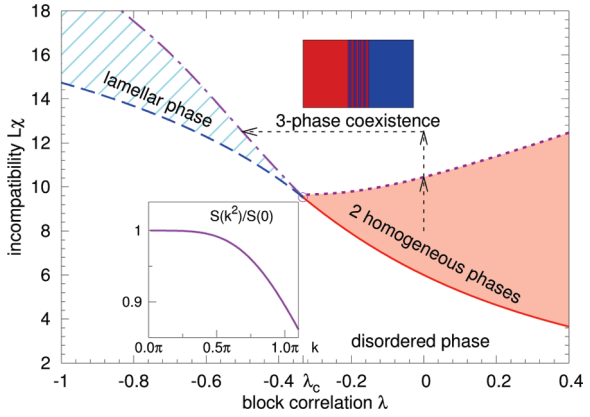

Figure 1. Phase diagram for triblocks with $M = 3$. Solid (red) curve: first macroscopic phase separation of disordered melt at $\lambda > \lambda_c$. Dotted (magenta) curve: for $\lambda > \lambda_c$, a lamellar phase shadow ($v = 0$) appears with finite k_0 and amplitude σ. Dot-dashed (purple) curve: boundary of three-phase coexistence toward system-spanning lamellae ($v = 1$) at $\lambda < \lambda_c$. Dashed (blue) curve: transition to a lamellar phase at $\lambda < \lambda_c$. A circle (○) marks the multicritical (Lifshitz) point. Bottom inset: global second-order structure function at the critical correlation $\lambda_c = -1/3$. Top inset: sketch of three-phase coexistence.

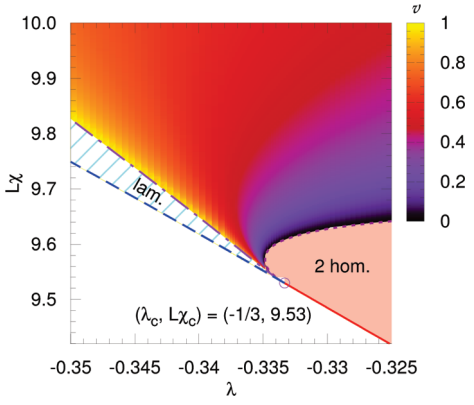

Figure 2. Volume fraction and boundaries of fractionated lamellae around multicriticality for triblocks with $M = 3$. Line styles as in Figure 1.

It can be verified that the new phase(s) set(s) in with zero volume fraction.[27]

Results and Discussion. The phase diagram for triblocks with $M = 3$ segments per block is shown in Figure 1. For $\lambda > \lambda_c = -1/3$, the first instability of the disordered melt is toward macroscopic phase separation due to the peak of the structure function at $k = 0$. On increasing the incompatibility $L\chi$ (bottom vertical arrow), one enters the three-phase region by crossing the dotted curve via a lamellar phase shadow with volume fraction $v = 0$. This fractionated shadow sets in with finite amplitude, and with *finite wavenumber*[27] because its copolymer-enriched sequence distribution deviates from the λ-defined one (see Figure 4). When one further increases $L\chi$ (along the top vertical arrow), the lamellar volume fraction grows. Now, keeping $L\chi$ constant and proceeding toward smaller values of λ (following the horizontal arrow), the volume fraction of the lamellae increases further. Eventually, for some $\lambda < \lambda_c$, the end of three-phase coexistence is reached (indicated by the dot-dashed curve), and lamellae take over to be the cloud phase with $v = 1$.

The wavenumber of the fractionated lamellae vanishes at the Lifshitz point, as does the wavenumber of system-spanning lamellae. However, as shown by the enlarged detail of

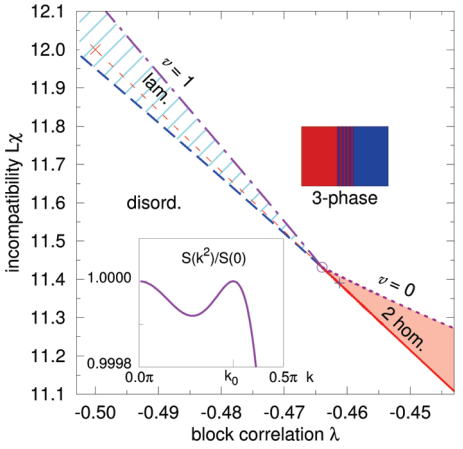

Figure 3. Phase diagram for continuous triblocks around multicriticality (λ_c, $L\chi_c$) = (−0.46400, 11.4316). Line styles as in Figure 1. Crosses mark the end points of the line of metastable homogeneous phase separations for $\lambda < \lambda_c$ (×) and of metastable lamellae for $\lambda > \lambda_c$ (+). Bottom inset: global second-order structure function at λ_c, with second peak at $k_0 = 0.3264\pi$ (in units of $3^{1/2}R_{ee}^{-1}$, with R_{ee} a chain's rms end-to-end distance).

the phase diagram with the lamellae's volume fraction v in Figure 2, the three-phase region is entered at two distinct χ values and thus with two distinct wavenumbers of the lamellar shadow for $\lambda \lesssim \lambda_c$. The lamellar shadow curve displays a *reentrant* behavior: it does not reach the Lifshitz point for $\lambda \downarrow \lambda_c$, but via a spiraling path invading the region $\lambda < \lambda_c$. Fractionation suppresses large-wavelength lamellae in the vicinity of the Lifshitz point, in favor of, first, macroscopic phases and, then, lamellae with finite wavelength, which however emerge at higher incompatibilities. On increasing incompatibility in the three-phase region, the lamellar wavelength decreases,[27] in agreement with previous mean-field calculations[3] but in contrast to results for one-component diblocks.[28]

What happens as the number M of segments per block increases? First, the critical block correlation λ_c, below which a nonzero maximum position of the global structure function $S(k^2)$ signals global microphase separation, decreases with increasing M. More remarkably, for $M \geq 7$, $S(k^2)$ features *two* peaks in the vicinity of λ_c. The peak at a finite wavenumber is lower than the peak at zero as long as $\lambda > \lambda_c$, reaching equal height at $\lambda = \lambda_c$ (see inset of Figure 3). Consequently, at multicriticality (λ_c,$L\chi_c$), the lamellar wavenumber attains a finite value *discontinuously*. Figure 3 shows the phase diagram for continuous triblocks, representative of the case $M \geq 7$. Here, the parameter region for three-phase coexistence close to multicriticality is larger than for $M < 7$: macroscopic phase separation no longer occurs for $\lambda < \lambda_c$, and thus the boundary curves show no reentrance. The double-peaked global structure function around multicriticality induces metastable lamellae in a small region $\lambda > \lambda_c$, where the free energy's absolute minimum indicates global macroscopic phase separation, and vice versa.

A composition triangle in Figure 4 visualizes sequence fractionation according to the phases' structures for continuous triblocks. Each corner represents one *sequence* class, a point within the triangle one sequence distribution. Because of the A−B exchange symmetry, the distributions of the two homogeneous phases coincide in this triangle. We show data for three representative, supercritical values of λ: $\lambda = 0$ (blue), $\lambda = -0.2$ (green), and $\lambda = -0.4$ (yellow). On the curve of λ-distributions, a solid symbol indicates the sequence distribution of the homogeneous cloud phase(s) at the onset

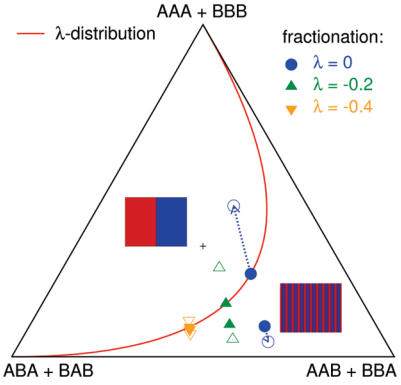

Figure 4. Sequence distribution triangle for random continuous triblocks at various block correlations. The diagram's center (+) corresponds to equal concentrations of all sequences ($p_\nu = {}^1/_3$, $\nu = 1, 2, 3$). Arbitrary distributions are represented as linear combinations of the vectors pointing from the center to the corners, each vector scaled with the concentration deviation $3(p_\nu - {}^1/_3)/2$. Distributions defined by λ lie on the (red) curve, λ ranging from −1 at the triangle's bottom left corner to +1 at its top. Solid symbols on this curve mark the sequence distribution of the cloud phase(s) (homogeneous phases for $\lambda > \lambda_c = -0.464$) at the onset of fractionation. Off-curve solid symbols mark the sequence distributions of the coexisting shadow phases (lamellar for $\lambda > \lambda_c$). Open symbols display the distributions of the coexisting phases at equal volume fractions ($v = 0.5$).

of fractionated three-phase coexistence. The solid symbol of the same color, to the bottom right of the curve, marks the distribution of the coexisting lamellar shadow phase (with zero volume fraction). The finite deviation of the lamellar shadow's sequence distribution from the λ-distribution identifies the transition to three-phase coexistence as discontinuous. On increasing the incompatibility, the lamellae's volume fraction increases, and their sequence distribution departs ever more from the λ-distribution (open symbols to the bottom right of the λ-curve display lamellae at 0.5 volume fraction). AAB/BBA as well as ABA/BAB sequences substantially accumulate in the lamellae. Moreover, since the ratio of these two sequence concentrations differs from the λ-defined ratio $p_2(\lambda)/p_3(\lambda)$, fractionated lamellae do not only expel homopolymers into the coexisting homogeneous phases.[27] As the volume fraction of the homogeneous, initial cloud phase(s) decreases, their distribution (at volume fraction 0.5 marked by open symbols to the top left) deviates increasingly from the λ-curve, showing a particular depletion in AAB/BBA sequences.

Conclusions. In conclusion, our minimal analytical model is able to resolve three-phase coexistence and provides insights into the mechanism of sequence selection among coexisting macroscopic and structured phases. At the multicritical point, lamellae in continuous triblocks display a *finite* wavenumber, contrasting with the known Lifshitz point behavior, here observed only for $M < 7$ segments per block. Work in progress analyzes this feature for systems with larger Q. An extension to fluctuation corrections would address the possible elimination of the multiphase coexistence at the Lifshitz point in favor of a structured, but disordered, microemulsion.

Acknowledgment. We thank Christian Wald for valuable advice. Financial support by the Deutsche Forschungsgemeinschaft via grant SFB-602/B6 is gratefully acknowledged.

References and Notes

(1) Hamley, I. W. *The Physics of Block Copolymers*; Oxford University Press: Oxford, 1998.
(2) Bates, F.; Fredrickson, G. H. *Annu. Rev. Phys. Chem.* **1990**, *41*, 525.

(3) Fredrickson, G. H.; Milner, S. T. *Phys. Rev. Lett.* **1991**, *67*, 835.
(4) Fredrickson, G. H.; Milner, S. T.; Leibler, L. *Macromolecules* **1992**, *25*, 6341.
(5) Bates, F.; Fredrickson, G. H. *Phys. Today* **1999**, *52*, 32.
(6) Nesarikar, A.; Olvera de la Cruz, M.; Crist, B. *J. Chem. Phys.* **1993**, *98*, 7385.
(7) Dobrynin, A. V.; Erukhimovich, I. Y. *J. Phys. I* **1995**, *5*, 365.
(8) Angermann, H.; ten Brinke, G.; Erukhimovich, I. Y. *Macromolecules* **1996**, *29*, 3255.
(9) Sfatos, C. D.; Shakhnovich, E. I. *Phys. Rep.* **1997**, *288*, 77.
(10) Semenov, A. N. *Eur. Phys. J. B* **1999**, *10*, 497.
(11) Subbotin, A. V.; Semenov, A. N. *Eur. Phys. J. E* **2002**, *7*, 49.
(12) Kuchanov, S. I.; Panyukov, S. V. *J. Phys.: Condens. Matter* **2006**, *18*, L43–L48.
(13) Flory, P. J. *Principles of Polymer Chemistry*; Cornell University Press: Ithaca, NY, 1953.
(14) Scott, R. L. *J. Polym. Sci.* **1952**, *9*, 423.
(15) Bauer, B. J. *Polym. Eng. Sci.* **1985**, *25*, 1081.
(16) Shakhnovich, E. I.; Gutin, A. M. *J. Phys.* (*Paris*) **1989**, *50*, 1843.
(17) Hornreich, R. M.; Luban, M.; Shtrikman, S. *Phys. Rev. Lett.* **1975**, *35*, 1678.
(18) Holyst, R.; Schick, M. *J. Chem. Phys.* **1992**, *96*, 7728.
(19) Brazovskiĭ, S. A. *Sov. Phys. JETP* **1975**, *41*, 85.
(20) Fredrickson, G. H.; Helfand, E. *J. Chem. Phys.* **1987**, *87*, 697.
(21) Sfatos, C. D.; Gutin, A. M.; Shakhnovich, E. I. *J. Phys. A* **1994**, *27*, L411.
(22) Gutin, A. M.; Sfatos, C. D.; Shakhnovich, E. I. *J. Phys. A* **1994**, *27*, 7957.
(23) Potemkin, I. I.; Panyukov, S. V. *Phys. Rev. E* **1998**, *57*, 6902.
(24) Janert, P. K.; Schick, M. *Macromolecules* **1997**, *30*, 3916.
(25) Houdayer, J.; Müller, M. *Europhys. Lett.* **2002**, *58*, 660.
(26) Houdayer, J.; Müller, M. *Macromolecules* **2004**, *37*, 4283.
(27) von der Heydt, A.; Müller, M.; Zippelius, A., to be published.
(28) Leibler, L. *Macromolecules* **1980**, *13*, 1602.
(29) In our minimal fractionation model, we ignore fluctuations within one phase and thus do not distinguish A-densities due to each sequence.[31]
(30) Equivalent to the scattering function in random phase approximation.[32]
(31) Erukhimovich, I. Y.; Dobrynin, A. V. *Macromol. Symp.* **1994**, *81*, 253.
(32) de Gennes, P. G. *Scaling Concepts in Polymer Physics*; Cornell University Press: Ithaca, NY, 1979.